Vibrational studies of the structural phase transition in caesium thiocyanate

1989 J. Phys.: Condens. Matter 1 7829

(http://iopscience.iop.org/0953-8984/1/42/005)

J. Phys.: Condens. Matter 1 (1989) 7829–7841. Printed in the UK

Vibrational studies of the structural phase transition in caesium thiocyanate

S Sathaiah, V N Sarin and H D Bist
Department of Physics, Indian Institute of Technology, Kanpur 208 016, UP, India

Received 20 September 1988, in final form 6 March 1989

Abstract. The room-temperature Raman and infrared (IR) spectra of caesium thiocyanate (CsNCS) and the temperature (T) dependence of the various thermo-sensitive bands are presented. On the basis of these detailed experimental studies the orthorhombic–cubic transition in CsNCS at $T_c \simeq 470$ K has been spectroscopically characterised as an order–disorder transition and to be first order in nature. Typical changes in the integrated intensity $I_{\nu_{C-N}}$ of the $\nu_{C-N} = 2042$ cm^{-1} mode of the Raman spectrum below T_c are represented as $I_{\nu_{C-N}} \propto (|T - T_c|)^{2\beta}$, with an order-parameter exponent $\beta \simeq 0.35$. These results are discussed in the context of a theory developed by Bruce *et al* to describe the Raman activity of hard modes near a structural phase transition. A remarkably consistent value of $\beta \simeq 0.35 \pm 0.02$ is obtained by expressing the squares of the frequency shifts of the NCS^- librational mode in the temperature range 300–453 K in terms of $(\nu_R^2 - \nu_0^2) \propto |T - T_c|^{2\beta}$, where $\nu_0 = \nu_R(T_c) = 125$ cm^{-1} and ν_R is the frequency of the in-plane rotatory mode. The anomalous increase in the band widths of many modes in the IR and Raman spectra closer to T_c may be attributed to increased anharmonicities as precursor effects to the transition. Above T_c the Raman spectrum due to the external modes is replaced by a broad-band spectrum and the fine structure ($\nu_{C-N} \pm$ external modes) in the ν_{C-N} region of the IR spectrum is smeared off. These results have been related to the loss of translational invariance and the emergence of dynamic disorder near T_c as both ions (Cs^+, NCS^-) are in motion.

1. Introduction

Structural phase transitions (SPT) in crystals between high-symmetry (disordered) and low-symmetry (ordered) phases have attracted the attention of both experimentalists and theoreticians for many years [1]. Raman, infrared (IR) and other vibrational spectroscopic studies provide deeper insight into the microscopic origin of the SPT.

In the Raman technique, light is scattered by fluctuations in the dielectric tensor of a material. Fluctuations of certain physical quantities are coupled to the fluctuations in the dielectric tensor; near phase transitions the fluctuations of some of these quantities are enhanced. This makes Raman scattering an important tool for the study of SPT, especially orientational order–disorder type transitions in ionic crystals [2]. In these substances ions order with a definite orientation below the transition temperature (T_c) and become uncorrelated above T_c. Because of their different orientations from cell to cell, the translational symmetry of the crystal is destroyed. The wavevector $\boldsymbol{k}$ need no longer be conserved in a light scattering process and phonons of any $\boldsymbol{k}$ that feel the disorder can contribute to the light scattering spectrum. In undergoing this order–disorder transition the crystal may change its structure.

0953-8984/89/427829 + 13 $02.50

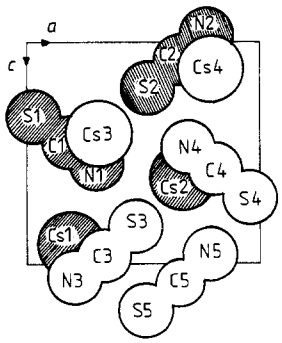

Figure 1. Arrangement of atoms in the orthorhombic unit cell. Shaded and unshaded atoms are at $y = \frac{1}{4}$ and $y = \frac{3}{4}$, respectively.

The alkali thiocyanates are ionic crystals that consist of spherical cations and rod-shaped anions. These substances are of interest because of their simpler structure and structural phase transitions at higher temperatures in which some of them adopt one of the alkali-halide structures through the orientational disorder of the anions. In this paper, we present the temperature dependence of Raman and IR spectra of caesium thiocyanate (CsNCS) in the temperature range 300 to about 475 K and spectroscopic characterisation of the order–disorder transition.

1.1. Crystal structure

At room temperature CsNCS has an ordered orthorhombic structure with space group D_{2h}^{16} (P*nma*). The primitive cell contains four formula units (i.e. $z = 4$) and the lattice parameters are $a = 7.978$ Å, $b = 6.332$ Å and $c = 8.332$ Å. The structure is layered along the b axis. In each unit cell two NCS^- ions lie on planes perpendicular to the b axis at $y = \frac{1}{4}$ and $y = \frac{3}{4}$; both cations and anions occupying sites of C_s symmetry. The adjacent thiocyanate ions in the same layer are almost perpendicular to one another (figure 1). Between 470 K and the melting point ($\simeq$480 K) CsNCS crystallises in a cubic structure similar to CsCl, with lattice constant $a_0 = 4.83$ Å, z = 1 and space group O_h^1 (Pm3m). Because of its existence in this very narrow temperature region ($\simeq$10 K), detailed dynamic information about the cubic phase is slightly difficult to acquire. X-ray, differential scanning calorimetry, differential thermal analysis and neutron diffraction studies identified the transition to be of order–disorder type and it has been characterised as first order on the basis of discontinuous changes in the volume and the latent heat of transformation [3–6]. Several room-temperature studies of vibrational spectra and lattice dynamics have been reported [7–13]. In this paper the vibrational spectral studies of the phase transition in a CsNCS sample are presented for the first time.

2. Experimental details

The CsNCS sample used for the present studies was an extra-pure sample from K and K Laboratories and it had been further purified by recrystallising three times from saturated aqueous solutions. The pure sample thus obtained was finely ground and used for the temperature dependence study of Raman spectra. Flat plate-like crystals with well developed (0 0 1) planes were obtained by slow evaporation of a saturated aqueous solution. These single crystals were properly polished to make very thin platelets and used for room-temperature and temperature-dependent IR spectral studies.

For the Raman measurements, linearly polarised 514.5 nm radiation from an argon-ion laser was used to excite the sample. A Spex 1403 double monochromator coupled with a photon counting system was used to record the spectra. For high-temperature studies a finely powdered CsNCS sample was positioned in the high-temperature cell. A Specac temperature controller with copper–constantan thermocouple touching the sample was used to measure the sample temperature with an accuracy of ±1 K. The average heating rate and the laser power employed at the sample were 1 K min^{-1} and 50 mW respectively.

For infrared measurements a thin single-crystal platelet was mounted on a special sample holder and fixed in the pallet holder of the Specac variable-temperature cell. The spectra were recorded using a Perkin-Elmer 580 double-beam grating infrared spectrometer. A Specac temperature controller in conjunction with a copper–constantan thermocouple was used to vary, control and measure the temperature of the sample with an accuracy of ±1 K.

3. Results

CsNCS is a typical ionic crystal in which the lattice structure is determined by the forces of at least two different strengths. The stronger overlap forces bind the N, C and S atoms together to form the rigid NCS^- ion, while the weaker long-range Coulomb forces mixed with some short-range forces bind the Cs^+ and NCS^- ions to form the CsNCS lattice. The lattice dynamics of this system can, to a first approximation, be described in terms of internal modes of intra-ionic NCS^- vibrations and external modes of inter-ionic motions.

3.1. Room-temperature Raman spectrum

The unpolarised Raman spectrum of the CsNCS sample at room temperature is shown in figure 2. The predominant bands in the low-frequency region below 200 cm^{-1} can be attributed to external modes and all other modes above 200 cm^{-1} correspond to internal modes. Peak positions, relative strengths and probable mode assignments for the external and internal modes are listed in table 1. The given symmetry assignments are those from the work of Ti *et al* [7]. In the external-mode region the band at 143 cm^{-1} (ν_R) is a rotatory mode that involves the hindered rotation of NCS^- about the *b* axis on the (0 1 0) plane. The band at 129 cm^{-1} is another rotatory mode, which involves the hindered libration out of the (0 1 0) plane. The band at 95 cm^{-1} is probably a two-phonon mode. All other low-frequency modes are translational modes. In the internal-mode region the two strong bands at 2042 and 2053 cm^{-1} are due to correlation field splitting of the C–N stretching mode ν_{C-N}. The band at ν_{C-S} = 750 cm^{-1} is the C–S stretching mode whereas δ_{N-C-S} = 475 and 486 cm^{-1} correspond to NCS^- bending modes. Bands at 950 and 975 cm^{-1} are overtones and the band at 963 cm^{-1} is a combination mode of δ_{N-C-S} fundamentals. The weak feature around 1494 cm^{-1} is an overtone of the ν_{C-S} fundamental. Other weaker features 742 (ν'_{C-S}), 2007 and 2027 cm^{-1} (ν'_{C-N}) are ν_{C-S}, ν_{C-N} modes of $N-^{13}C-S^-$ and $^{15}N-C-S^-$ isotopic species. The overtones of NCS^- bending modes have higher peak intensities (≃5 times) compared to their fundamentals, indicating anharmonic effects even at room temperature.

Table 1. Vibrational wavenumbers, relative strengths, mode assignments and symmetry species of Raman-active modes in CsNCS observed at 300 K†.

(*a*) External and internal modes.

	External modes							Internal modes				
Peak wavenumbers (cm^{-1})	38	45	55	73	95	130	143	475	486	750	2042	2053
Relative strengths	s	s	m	vs	s	ms	ms	vw	vw	s	vs	ms
Mode assignments	T	T	T	T	Two-phonon	R	R	δ^{a}_{N-C-S}	δ^{b}_{N-C-S}	ν_{C-S}	ν_{C-N}	ν_{C-N}
Symmetry species‡	A_g	(A_g, B_g)	B_g	B_g	?	B_g	(A_g, B_g)	(A_g, B_g)	(A_g, B_g)	(A_g, B_g)	A_g	A_g

(*b*) Multi-phonon modes and internal modes of isotopic species.

	Multi-phonon modes				Internal modes of isotopic species					
Peak wavenumbers (cm^{-1})	951	963	975	1494	742	746	2002	2007	2022	2027
Relative strengths	w	vw	mw	vw	m	m	w	m	w	m
Mode assignments	$2\delta^{a}_{N-C-S}$	$\delta^{a}_{N-C-S} + \delta^{b}_{N-C-S}$	$2\delta^{b}_{N-C-S}$	$2\nu_{C-S}$	ν_{C-S} and ν_{C-N} modes of N–^{13}C–S and ^{15}N–C–S isotropic species					

† The abbreviations v, s, m and w stand for very, strong, medium and weak (peak intensities); R and T stand for rotational and translational modes. ν_{C-N}, δ_{N-C-S} and ν_{C-S} denote the C–N stretching, N–C–S^- bending and C–S stretching modes of N–C–S^- in that order.
‡ Inferred from [7].

Table 2. Vibrational wavenumbers and tentative assignments of IR-active internal modes and multi-phonon modes (overtones and combinations).

Peak wavenumbers (cm^{-1})	Internal modes				Multi-phonon modes†					
	488	758	750‡	2050	957, 980	1927	1982	2092	2128	2180
Mode assignments	$\delta_{N\text{-}C\text{-}S}$	$\nu_{C\text{-}S}$	$\nu\,^{13}_{C\text{-}S}$	$\nu_{C\text{-}N}$	$\delta'_{N\text{-}C\text{-}S} + \delta''_{N\text{-}C\text{-}S}$	$\nu_{C\text{-}N} - 123$	$\nu_{C\text{-}N} - 68$	$\nu_{C\text{-}N} + 42$	$\nu_{C\text{-}N} + 78$	$\nu_{C\text{-}N} + 130$
External mode wavenumbers (cm^{-1})						($\nu_R = 130$)	($\nu_T = 73$)	($\nu_T = 45$)	($\nu_T = 73$)	($\nu_R = 130$)

† There are also very broad bands at 1428, 1680, 1768, 2865, 3100 and 3210 cm^{-1}; the spectral features at 830, 893, 1025, 1095, 1198, 1238, 1500 and 2550 cm^{-1} also correspond to multi-phonon modes.

‡ $\nu\,^{13}_{C\text{-}S}$ is the $\nu_{C\text{-}S}$ mode of N–^{13}C–S isotopic species.

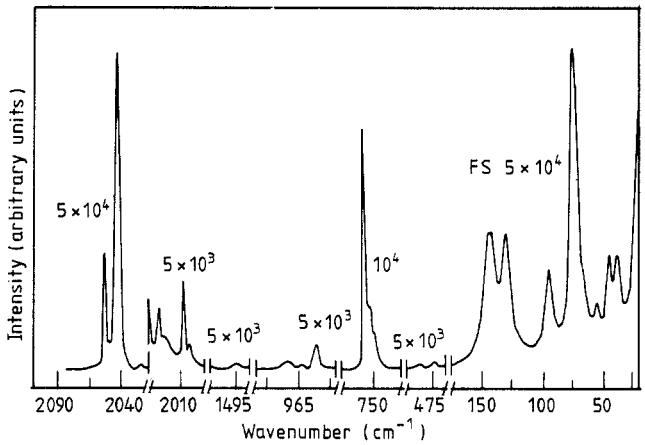

Figure 2. Unpolarised Raman spectrum of CsNCS single crystal at room temperature. FS 5×10^4, 5×10^3 and 1×10^4 are recording sensitivities (photon counts per second).

3.2. Room-temperature infrared data

The unpolarised transmission IR spectrum of the CsNCS thin single-crystal platelet is given in figure 3. Peak positions and tentative assignments of all the observed bands are listed in table 2. The dominant bands around 488, 758 and 2050 cm^{-1} are NCS^- bending, C–S stretching and C–N stretching modes, respectively. All other broader and weaker features correspond to multi-phonon processes. Attempts have been made to explain the observed complex fine structure in the C–N stretching region of the infrared spectrum (figure 3), on the basis of multi-phonon processes involving $\nu_{C-N} \pm$ external modes.

3.3. Temperature dependence of Raman spectra

Raman spectra in the C–N stretching region of CsNCS powder are shown in figure 4(*a*), for 10 typical temperatures between 299 and 465 K. On increasing the temperature the peak intensities of (2042, 2053 cm^{-1}) ν_{C-N} modes decrease monotonically, with marginal changes in half-widths, but there are no appreciable changes in their peak positions till 440 K. Around 446 K a broad wing appears on the higher-frequency side of the ν_{C-N} modes. As the temperature increases further, the band widths of ν_{C-N} modes increase exponentially. The higher-frequency wing enhances in intensity at the expense of a decrease in the peak intensities of the main ν_{C-N} modes. Finally around 461 K the complete C–N stretching region is replaced by a single broad ($\simeq$7 times broader than ν_{C-N} modes) band peaked around 2059 cm^{-1}. For temperatures higher than 461 K this broad band also starts to decrease in peak intensity. Typical changes in the integrated intensity $I_{\nu_{C-N}}$ and FWHM (full width at half maximum) γ_{C-N} of the ν_{C-N} (at 2042 cm^{-1}) mode with temperature are plotted in figure 5(*a*). Integrated intensity decreases continuously in a well defined manner in the temperature range 300–458 K, and by extrapolating the curve it becomes zero around 463 K. Assuming this value as the approximate transition temperature (T_c), a plot of log $I_{\nu_{C-N}}$ versus log$|T - T_c|$ (figure 5(*b*)) for $5 \leqslant |T - T_c| \leqslant 95$ K gives a perfect straight line with a slope of 0.69 ± 0.04. So the strong variation in the integrated intensity with temperature can be represented as $I_{\nu_{C-N}} \propto (|T - T_c|)^{2\beta}$ with an order-parameter exponent $\beta \simeq 0.35 \pm 0.02$. This characteristic behaviour has been verified by repeating the experiment. The β-value obtained

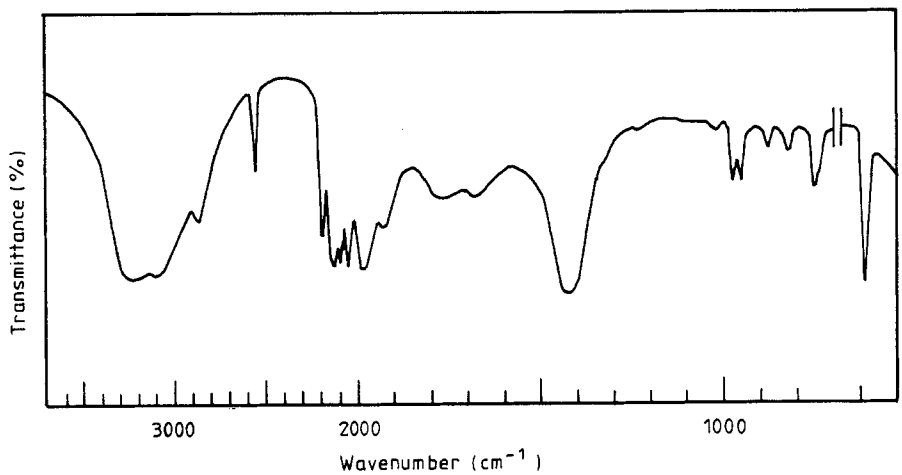

Figure 3. Unpolarised transmission IR spectrum of CsNCS single-crystal platelet at room temperature.

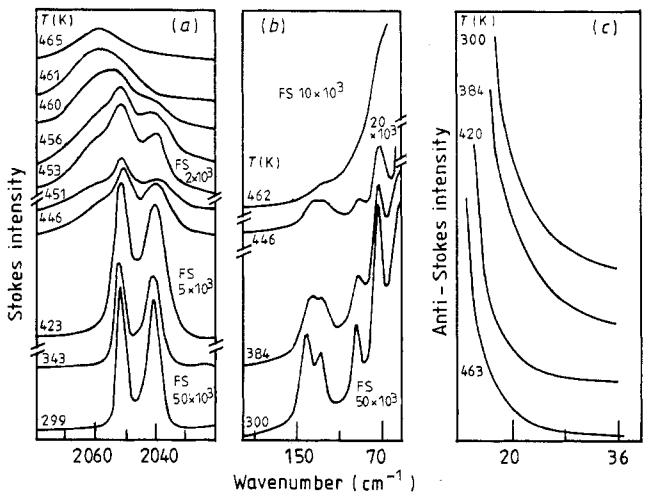

Figure 4. Thermo-sensitive mode regions in the Raman spectrum of CsNCS polycrystalline sample. Temperature dependence of Raman spectra in (*a*) C–N stretching region, (*b*) lattice-mode region and (*c*) Rayleigh wing (on the anti-Stokes side of the Raman spectrum).

in the repeated experiment is $\beta \simeq 0.36 \pm 0.02$. The band width γ_{C-N} increases linearly until 440 K and exponentially near the transition temperature. Peak frequencies of ν_{C-N} modes remained constant throughout the temperature range studied (figure 6(*a*)).

Figure 4(*b*) shows typical changes in the external-mode (50–200 cm^{-1}) region. Apart from small changes in the peak positions and band widths and a decrease in their peak intensities, the lattice mode structure does not change appreciably until ($T<$) 446 K. For temperatures above 446 K the continuous broadening of all the bands, and finally around 462 K the replacement of the complete lattice spectrum by a broad-band spectrum with a small hump around 125 cm^{-1}, can be seen. Plots of peak frequencies of the lattice modes ν_i versus temperature are given in figure 6(*b*). The peak frequencies of all the lattice modes decrease monotonically. The in-plane rotatory mode displays the

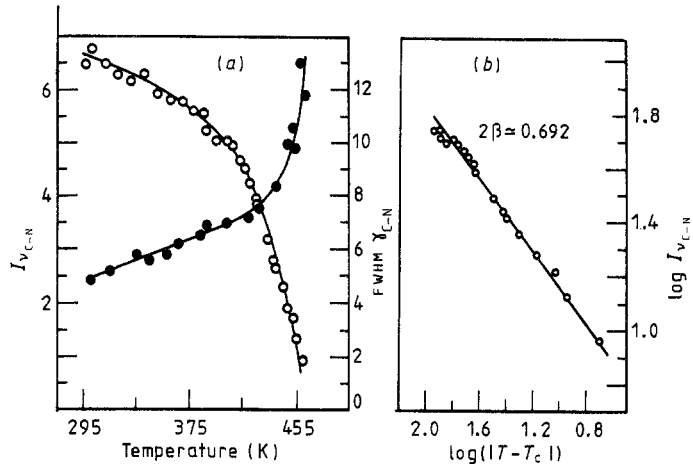

Figure 5. (*a*) Variations in the integrated intensity $I_{\nu_{C-N}}$ (○) and FWHM γ_{C-N} (cm^{-1}) (●) of C–N stretching mode with temperature. (*b*) Plot of log $I_{\nu_{C-N}}$ versus log$|T - T_c|$ for $5 \leq |T - T_c| \leq 95$ K.

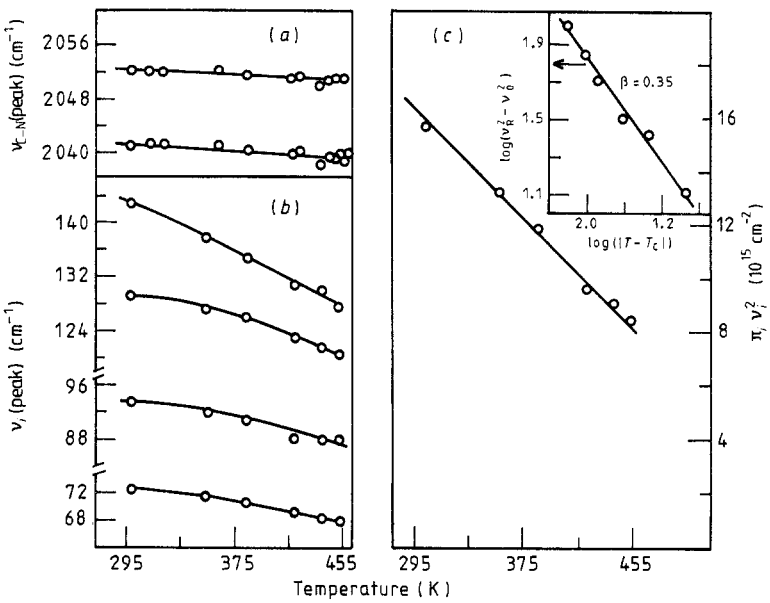

Figure 6. Changes in the peak frequencies with temperature: (*a*) ν_{C-N} modes versus temperature; (*b*) lattice modes ν_i versus temperature; (*c*) product of squares of frequencies $\pi_i \nu_i^2$ for four lattice modes (ν_i) versus temperature. The inset shows a plot of $\log(\nu_R^2 - \nu_0^2)$ versus $\log(|T - T_c|)$ in the T range 300–453 K for a librational mode (ν_R).

largest softening of 11% (at 453 K). The out-of-plane rotatory mode softens by 7% and all other translational modes by 6%. It is interesting to note that the squares of the frequency shifts of the in-plane rotatory mode (ν_R) in the temperature range 300–453 K vary as $(\nu_R^2 - \nu_0^2) \propto |T - T_c|^{2\beta}$, with $\beta \simeq 0.35 \pm 0.02$, $\nu_0 = \nu_R(T_c) = 125\,cm^{-1}$ and $T_c \simeq 462$ K. Log$(\nu_R^2 - \nu_0^2)$ versus log$|T - T_c|$ gives an exact straight line (see the inset in

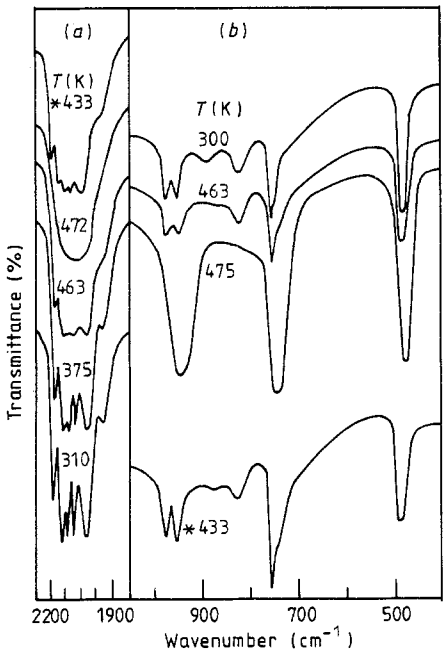

Figure 7. Temperature dependence of IR spectra in (*a*) C–N stretching (1850–2300 cm^{-1}) region and (*b*) 400–1050 cm^{-1} region. The spectra at 433 K (marked with an asterisk (*)) correspond to the data obtained during the cooling cycle.

figure 6(*c*)) with a slope of 0.7 ± 0.04. For the other lattice modes, ν_i^2 do not change linearly with temperature but the product of squares $\pi_i \nu_i^2$ of external modes (including ν_R^2) follows an exact linear relationship. Figure 6(*c*) is a plot of $\pi_i \nu_i^2$ versus T showing a straight line in the temperature range 300–453 K. We verified this behaviour by repeating the experiment. Typical changes in the Rayleigh wing (on the anti-Stokes side of the spectrum) with temperature are shown in figure 4(*c*). As the sample temperature increases, the Rayleigh wing slowly narrows down, and finally a sharper wing can be seen around 463 K. All the observed changes in the Raman spectra of polycrystalline CsNCS during the heating cycle are also observable in the cooling cycle but with a large hysteresis of about 35 K. This large hysteresis (≈35 K) in the transition temperature is consistent with the value of about 45 K reported from x-ray results (figure 2 in [3]) and the value of about 40 K from our IR data.

3.4. Temperature variation of the infrared data

As the temperature increases above 300 K the gradual broadening and smearing of fine structure in the C–N stretching region can be clearly seen from figure 7(*a*). Finally around 472 K it is completely smeared off and a single broad band can be seen for temperatures above 472 K. This behaviour is consistent with our Raman results, where the low-frequency external-mode region is replaced by a broad-band spectrum for temperatures above 462 K. The IR spectra in the C–S stretching and NCS^- bending (400–1050 cm^{-1}) region are shown in figure 7(*b*), for four different temperatures below and above the transition temperature. Apart from small changes in the band widths and peak intensities, the spectra do not change much till 463 K. In fact the IR spectrum at 463 K is identical to that at room temperature. For temperatures 5–10 K above 463 K, an anomalous increase in peak intensities and half-widths of the C–S stretching and NCS^- bending modes can be seen. Similarly overtones of NCS^- bending fundamentals

merge into a single broader band with stronger peak intensity. Similar broadening is observed for all other multi-phonon modes and some of the weaker multi-phonon bands become too broad to observe. The characteristically different spectrum around 475 K, consisting of very broad bands, indicates the highly disordered nature of the high-temperature phase I. In the cooling cycle this phase I persisted until 433 K (denoted by the asterisk (*) in figure 7(*b*)), showing a large hysteresis of 40 K in the transition temperature.

4. Discussion

All the changes in the Raman spectra above 463 K, e.g. the replacement of the external-mode region by a broad-band spectrum, the appearance of a very broad band around 2059 cm^{-1} in place of (2042, 2053 cm^{-1}) C–N stretching modes and the characteristic changes in the integrated intensity, reveal an order–disorder transition around that temperature. The changes in the IR spectra indicate the transition temperature to be at 472 ± 1 K, in agreement with the reported $T_c \simeq 470$ K from x-ray, neutron diffraction and thermal investigations [3–6]. The discrepancy in the observed T_c value in our Raman measurements can be attributed to local heating effects, i.e. the laser-irradiated spot temperature of the sample is about 7 K higher than the measured one at a slightly different point.

4.1. First-order nature of the transition

At room temperature the two ν_{C-N} modes (2042 and 2053 cm^{-1}) in the Raman spectrum are due to correlation field splitting. So the replacement of these ν_{C-N} modes by a single broad band (2059 cm^{-1}) can be attributed to the apparent decrease in the anisotropy of the crystal field around the NCS^- ion, which probably occurs as a result of the disordering oscillations of the NCS^- ion near T_c. Then the simultaneous appearance of both the broad band at 2059 cm^{-1} (characteristic of disordered phase I) and the 2042 and 2053 cm^{-1} modes (characteristic of low-temperature ordered phase II) in the temperature range 446–462 K indicates the coexistence of both phases in that range. Such coexistence phases are also seen in IR spectral studies during a cooling cycle. In the heating cycle there are marginal changes in the IR spectra (of phase II) until 463 K. However, an increase in the temperature by 5–10 K above 463 K results in a spectrum consisting of anomalously broad and stronger bands characteristic of the highly disordered nature of phase I. In the cooling cycle this phase I persisted up to 433 K as a metastable phase. All these observations, i.e. the coexistence phases, large hysteresis in the T_c value and sudden changes in the IR spectra within a small temperature range, are characteristic features of a first-order transition.

4.2. Spectral manifestation of disorder

As mentioned earlier, x-ray studies identified phase I to be cubic and a 24-fold orientational disordered arrangement of the NCS^- ion was postulated in order to fulfil the symmetry requirements of the cubic phase. The spectral manifestations of this highly disordered character of phase I can be seen from our observations above T_c, i.e. the appearance of a broad wing in the lattice-mode region of Raman spectra and smeared-off fine structure in the C–N stretching region of IR spectra, which could occur due to

the breakdown of $\boldsymbol{k} = 0$ selection rules. The absence of discrete Raman lines in the lattice region confirms its cubic structure. Since first-order Raman scattering in the CsCl-like cubic phase is not allowed by group theory, the broad feature around 125 cm^{-1} may be associated with disorder-allowed phonons.

4.3. Generalised soft-mode-like behaviour of external modes

Some of the observations in our Raman studies (e.g. gradual narrowing of Rayleigh wing with temperature, finally becoming sharper above T_c, and the broad-band lattice spectra in phase I) look strikingly similar to that reported by Dultz [14] for the disordered cubic phase of KCN. Assuming some similarity between transitions in KCN and CsNCS, Irving *et al* [5] concentrated their neutron diffraction studies of CsNCS on acoustic modes in an attempt to find soft modes associated with the transition. But they did not observe any such mode from their studies. Our Raman results also show that all the external modes are temperature-dependent to some extent, but none of them individually show purely soft-mode-like behaviour. Interestingly the product of the squares of these external modes, $\Pi_i \nu_i^2$, varies linearly in the temperature range 300–453 K as shown in figure 6(*c*). By extrapolating the curve, $\Pi_i \nu_i^2$ becomes zero around 600 K, which is considerably higher than the observed T_c value (i.e. 463 K). A similar type of behaviour had been reported by Iqbal *et al* [15] for KNCS in which the reported order–disorder transition temperature was 413 K and the extrapolated temperature where $\Pi_i \nu_i^2$ becomes zero was 535 K. For $NaClO_3$ crystal Rao *et al* [16] reported a similar relation, i.e. $\Pi_i \nu_i^2 \propto (T - T_c)$, with an extrapolated $T_c = 593$ K (greater than the melting point 537 K) for the first-order transition, and their Raman results were comparable with dielectric measurements. These authors interpreted the linear behaviour of $\Pi_i \nu_i^2$ versus T as the generalisation of Cochran's soft-mode concept. In this line of thought $\Pi_i \nu_i^2$ not becoming zero at T_c in CsNCS may be due to the highly first-order nature of the transition, the sample might have distorted to another phase before $\Pi_i \nu_i^2$ had a chance to go to zero. To confirm the applicability of this generalised soft-mode concept, one also has to observe a linear increase in $\Pi_i \nu_i^2$ with temperature above T_c. This could not be verified in the present case due to the resulting broad-band lattice spectrum above T_c. Additionally, the T dependences of all the lattice modes, including the weaker modes below 60 cm^{-1}, have to be considered in $\Pi_i \nu_i^2$.

On the other hand, the peculiar variations $(\nu_R^2 - \nu_0^2) \propto (|T - T_c|)^{0.7}$ in the librational mode for T ($\leqslant$453 K) well below T_c may probably be associated with the transition. Although ν_R remains as a weak diffusive structure around 125 cm^{-1} ($= \nu_0$) above T_c, this type of softening may not be unusual for the transition triggered by reorientational fluctuations of the ions. Further work along these lines is in progress.

4.4. Calculation of order-parameter exponent β

It is interesting to note that the integrated intensity $I_{\nu_{C\text{-}N}}$ falls off ($I_{\nu_{C\text{-}N}} \propto (|T - T_c|)^{2\beta}$ for $T \rightarrow T_c - 5$ K from below) like the square of the order parameter (η^2), giving an order-parameter exponent $\beta \simeq 0.35 \pm 0.02$. Recently Bruce *et al* [17] have developed a general theory for the onset of Raman activity of hard modes (modes that are not directly involved in the phase transition) near a SPT. These hard modes are of interest if, on symmetry grounds, they are Raman-active below T_c and Raman-inactive above T_c.

According to this theory, the total Raman intensity I for such modes can be expressed as

$$I = I^{LR} + I^{CP} + I^{PH} \tag{1}$$

where I^{LR} represents the long-range conribution to the first-order scattering in phase II and is proportional to the square of the order parameter (η^2); I^{CP} is the central peak contribution resulting from the first-order hard-mode scattering induced by short-range order; and I^{PH} represents the contributions from two-phonon processes involving hard- and soft-phonon quasi-harmonic interactions and giving rise to second-order Raman scattering. The expression (1) has been used to explain the temperature dependence of Raman intensities of hard modes near the tetragonal to cubic (continuous with first-order components) transitions in $KMnF_3$ and $RbCaF_3$ samples [17]. In CsNCS sample the temperature dependence of the integrated intensity $I_{\nu_{C-N}}$ of the ν_{C-N} mode (for T well below T_c) is remarkably consistent with the dominance of the first term in equation (1). So in the low-temperature phase the Raman intensity of the ν_{C-N} mode may solely be controlled by the long-range order. It is difficult to draw any quantitative conclusions for temperatures very close to T_c because of the broad-band spectra and first-order nature of the transition. However, the consistent value of $\beta \simeq 0.35 \pm 0.02$ from librational mode frequency shifts (for T well below T_c) gives additional support to the above results.

4.5. Phase transition mechanism

Deep in the ordered phase the linear increase in the band width of the ν_{C-N} mode can be understood as cubic anharmonic contributions to its half-width. Neutron diffraction studies of CsNCS sample [5, 6] revealed an anomalous increase in the mean-square displacements of both the Cs^+ and SCN^- ions near T_c and this highly anharmonic behaviour was attributed to precursor effects associated with the transition. In the vicinity of the transition the anomalous increase in the band widths of many modes in the IR and Raman spectra, especially γ_{C-N} of the ν_{C-N} mode in the Raman spectrum, may be associated with these strongly enhanced anharmonicities near T_c. The large entropy change associated with the transition, 5.7 eu† mol^{-1} (almost twice the melting entropy, 3.0 eu mol^{-1} [3]), and the anomalous broad features in the IR and Raman spectra above T_c, suggest that the high-temperature cubic phase is a classic 'plastic crystalline phase' [18].

The transition in CsNCS may be compared with that of a KNCS sample, which also has an orthorhombic layer structure (space group P*bcm*) at room temperature but transforms at 414.5 K to a tetragonal structure (space group I4/mcm). The transition in KNCS has been determined to be second order in character, with a small first-order component. Near the transition temperature NCS^- ions in KNCS are believed to undergo dynamic reorientational fluctuations between two energetically equivalent positions [15, 19–22]. One can expect thermodynamically similar transitions in rubidium, ammonium and thallium thiocyanates whose low-temperature phase II structures are known to be (orthorhombic) isomorphous to that of KNCS. But the transition in CsNCS is found to be completely different. The large entropy change at T_c, the first-order character of the transition, the cubic symmetry and the highly disordered nature of phase I are unique features of the CsNCS sample among all the alkali thiocyanates. Although

† Entropy unit (cal deg^{-1}).

the measured change in entropy, 5.7 eu mol^{-1}, is close to $R \ln 24 = 6.3$ eu mol^{-1}, supporting the 24-fold orientational disordered arrangement of NCS^- ions in phase I, the large increase in the band widths of almost all the bands in the IR and Raman spectra near T_c and the temperature dependence of all the observed lattice modes suggest that the transition may not be solely related to NCS^- ion disorder but probably involves shifts of both ions (Cs^+, NCS^-). This mechanism for the phase transition involving a cooperative dynamic reorientational disordering near T_c as both ions are in motion is consistent with the previously reported neutron diffraction results.

Acknowledgment

The authors would like to thank the Department of Science and Technology, Government of India, for providing a grant to equip the laboratory with the instruments used in the present study.

References

[1] Scott J F 1974 *Rev. Mod. Phys.* **46** 83–128
[2] Wang C H 1984 *Vibrational Spectroscopy of Phase Transitions* ed. Z Iqbal and F J Owens (New York: Academic) p 153
[3] Manolatos S, Tillinger M and Post B 1973 *J. Solid State Chem.* **7** 31–5
[4] Klement W Jr 1976 *Bull. Chem. Soc. Japan* **49** 2148–53
[5] Irving M A, Elcombe M M and Smith T F 1985 *Aust. J. Phys.* **38** 85–95
[6] Moss B K, Mair S L, Mcintyre C J and McMullan R K 1987 *Acta Crystallogr.* B **43** 16–23
[7] Ti S S, Kettle S F A and Ra Ø 1977 *Spectrochim. Acta* A **33** 111–19
[8] Ra Ø, Ti S S and Kettle S F A 1978 *J. Chem. Phys.* **68** 2638
[9] Ti S S and Ra Ø 1980 *J. Chem. Phys.* **73** 5738–48
[10] Ti S S and Ra Ø 1980 *J. Chem. Phys.* **73** 5749–52
[11] Irving M A, Prawer S, Smith T F and Finlayson T R 1983 *Aust. J. Phys.* **36** 85–92
[12] Irving M A, Elcombe M M and Smith T F 1984 *Aust. J. Phys.* **37** 287–304
[13] Hua G and Ninio F 1986 *Aust. J. Phys.* **39** 309–27
[14] Dultz W 1974 *Solid State Commun.* **15** 595–8
[15] Iqbal Z, Sarma L H and Moller K D 1972 *J. Chem. Phys.* **57** 4728
[16] Rao A D P, Katiyar R S and Porto S P S 1972 *Phys. Rev. Lett.* **28** 665–8
[17] Bruce A D, Taylor W and Murray A F 1980 *J. Phys. C: Solid State Phys.* **13** 483–504
[18] Sherwood J N 1979 *The Plastically Crystalline State* (New York: Wiley)
[19] Sakiyama M, Suga H and Seki S 1963 *Bull. Chem. Soc. Japan* **36** 1025–32
[20] Yamada Y and Watanabe T 1963 *Bull. Chem. Soc. Japan.* **36** 1032–7
[21] Owens F J 1979 *Solid State Commun.* **29** 789–91
[22] Karpov S V, Khassan Ali A V and Shultin A A 1982 *Sov. Phys.–Solid State* **24** 39–41